



The coupled Hf-Nd isotope record of the early Earth in the Pilbara Craton



R. Salerno^{a,*}, J. Vervoort^a, C. Fisher^{a,b}, A. Kemp^b, N. Roberts^c

^a School of the Environment, Washington State University, Pullman WA, 99164, USA

^b School of Earth Sciences, University of Western Australia, Crawley 6009, Australia

^c Department of Geoscience, University of Wisconsin-Madison, Madison WI, 53706, USA

ARTICLE INFO

Article history:

Received 19 February 2021

Received in revised form 14 July 2021

Accepted 27 July 2021

Available online 13 August 2021

Editor: F. Moynier

Keywords:

Archean

Pilbara

Hf and Nd isotope decoupling

Sm-Nd geochronology

titanite

apatite

ABSTRACT

Initial Hf and Nd isotope compositions of Earth's oldest rocks provide essential information on the differentiation of the Earth into enriched crustal and depleted mantle reservoirs in its early history. The majority of Eo-Paleoarchean rocks worldwide, however, have isotope compositions that appear to be decoupled: initial Hf isotope compositions, determined on zircon, are broadly chondritic with little variation; initial Nd isotopes on bulk rocks, in contrast are highly variable with both supra- and sub-chondritic compositions. Most of these studies are from polymetamorphic terranes where the potential for disturbance of the isotope system is high. This is particularly true for the Sm-Nd system where more easily altered REE-rich accessory phases are the major repositories for these elements.

In order to better understand crust-mantle evolution during the Archean—and to address the issue of Hf and Nd isotope decoupling—we examine a suite of well-preserved Paleoproterozoic granites from the Pilbara Craton. Our approach integrates the initial Hf isotope composition and U-Pb ages of zircon, the initial Nd isotope compositions of titanite and apatite, and U-Pb ages of titanite by laser ablation split stream (LASS) analysis. The zircon and titanite U-Pb data yield crystallization ages of 3.47 to 3.28 Ga, in good agreement with the combined apatite-titanite-WR Sm-Nd isochron ages of each sample, demonstrating that both the U-Pb and Sm-Nd systems have not been modified since igneous crystallization. The initial Hf isotope compositions of zircon from all samples are broadly chondritic with $\varepsilon_{\text{Hf}(i)}$ values of -0.3 to $+0.8$, in agreement with the bulk-rock Hf. The initial Nd isotope compositions of the titanite and apatite are also broadly chondritic ($\varepsilon_{\text{Nd}(i)}$ titanite, -1.0 to $+2.0$; apatite, -0.6 to $+0.9$) and agree with the Nd isotope composition of the bulk-rock ($\varepsilon_{\text{Nd}(i)} = +0.2$ to $+1.2$) and the initial $^{143}\text{Nd}/^{144}\text{Nd}$ ratios determined from the titanite-apatite-WR isochrons ($\varepsilon_{\text{Nd}(i)} -0.9$ to $+1.3$).

From these data, we make two fundamental observations. First, the granites in this study were derived from a source that was chondritic with respect to both Hf and Nd isotopes from 3.47 to 3.28 Ga; neither system supports the presence of either a strongly depleted mantle or enriched crustal source. Second, the Lu-Hf and Sm-Nd isotope systems in the Pilbara samples are in full agreement. This stands in stark contrast to the record of rocks from Eo-Paleoarchean terranes of higher metamorphic grade, where the Hf and Nd isotope compositions have been “decoupled”. This further underscores the importance of recognizing potential effects of high-grade metamorphism on the Sm-Nd bulk-rock record. The integrated age-isotope approach taken here illustrates a way to assess the integrity of bulk-rock Nd isotope data through examination of the Sm-Nd isotope systematics of the LREE-rich accessory minerals in rocks.

© 2021 Elsevier B.V. All rights reserved.

1. Introduction

Samarium-neodymium and lutetium-hafnium isotope systematics have long been utilized to understand the differentiation of Earth's crust and mantle into incompatible-element enriched and

depleted reservoirs (DePaolo, 1981; McCulloch and Bennett, 1994). In both isotope systems, the daughter isotope is more incompatible than the parent, leading to higher Sm/Nd and Lu/Hf ratios in crustal reservoirs and, conversely, lower ratios in the depleted mantle. The analogous geochemical behavior of these isotope systems has also resulted in the positive correlation of $^{176}\text{Hf}/^{177}\text{Hf}$ and $^{143}\text{Nd}/^{144}\text{Nd}$ that is recognized in nearly all terrestrial materials (e.g., the “terrestrial array”; Vervoort et al., 1999). In the ancient rock record, however, this positive correlation between Hf and Nd

* Corresponding author.

E-mail address: ross.salerno@wsu.edu (R. Salerno).

isotopes has been shown to break down, where large variations in whole-rock Nd isotope ratios are not mirrored in the Hf isotope system, as captured by zircon (e.g., Vervoort et al., 1996).

The Nd isotope record of Eo-Paleoarchean rocks globally documents both strongly positive and negative initial ε_{Nd} values (e.g., Bennett et al., 1993; Bowring and Housh, 1995). The positive initial ε_{Nd} values have been used to argue for the formation of an extensive depleted mantle reservoir very early in Earth's history (e.g., Bennett et al., 1993). The negative ε_{Nd} values are interpreted to record the presence of a complementary, incompatible element enriched crustal reservoir (e.g., Bowring and Housh, 1995).

The Hf isotope record is markedly different. Initial Hf isotope compositions of zircon from Eo-Paleoarchean granitic rocks in the Pilbara Craton, Saglek Block and Nuvvuagittuq belt in the North Atlantic Craton, the Minnesota River Valley gneiss in the Superior Craton, the Ancient gneiss in the Kaapvaal Craton, and the Limpopo belt are all broadly chondritic (e.g., Zeh et al., 2007; Kemp et al., 2009; O'Neil et al., 2013; Petersson et al., 2020). Magmatic portions of zircon crystals in the oldest rocks (Acasta Gneiss Complex) and the most ancient detrital zircons (from the Jack Hills metaconglomerate), have chondritic to moderately subchondritic Hf isotope compositions for the oldest samples with a trend that is increasingly subchondritic with decreasing age (e.g., Kemp et al., 2010; Bauer et al., 2017).

The broadly chondritic Hf isotope character of the early Earth record is interpreted as representing crust extracted from a chondritic mantle that persisted until ~ 3.8 Ga (e.g., Fisher and Vervoort, 2018). The subchondritic compositions suggest occurrence of enriched crustal material that was subsequently reworked (e.g., Kemp et al., 2010). The lack of strongly positive initial ε_{Hf} values in the Eoarchean has been used to argue against development of an extensive depleted mantle reservoir in the early Earth (e.g., Fisher and Vervoort, 2018).

These data illustrate a fundamental disagreement between the Hf and Nd isotope records in the early Earth: the Hf isotope record from zircon and well-preserved bulk rocks is broadly chondritic; Nd isotope compositions, determined from bulk rock samples, vary significantly from supra- to sub-chondritic. Thus, the close correlation of Hf and Nd isotope compositions in the full range of crust and mantle materials that defines the Terrestrial Hf-Nd array throughout most of Earth's history (Vervoort et al., 1999) does not hold for many of these ancient samples. This conflicting isotope record has been described as "decoupled" (e.g., Caro et al., 2005) or as the Hf-Nd paradox (e.g., Vervoort, 2014).

Several possibilities have been suggested to explain the conflicting datasets. For example, Caro et al. (2005) and Rizo et al. (2011) proposed that decoupling of Hf and Nd isotopes arises from the role of a Mg-perovskite rich cumulate formed in the deep mantle during crystallization of an early magma ocean. The basis for this inference is that Hf is more compatible than Lu in Mg-perovskite, resulting in a residual mantle with higher Sm/Nd but lower Lu/Hf that evolves to positive ε_{Nd} but chondritic-to-negative ε_{Hf} .

A simpler explanation for the Hf-Nd paradox, however, is that these old rocks were affected by open system behavior sometime after their initial crystallization during which their Sm-Nd isotope systematics were modified (e.g., Moor bath et al., 1997; Hammerli et al., 2019). Unlike Hf isotopes in zircon, the early Earth Sm-Nd isotope record has been determined from bulk rock samples, often lacking precise magmatic crystallization age constraints, and which have potential for cryptic disturbances that may go unrecognized. Moreover, the Sm-Nd budget of many crustal rocks are controlled by LREE-rich phases such as apatite, monazite, allanite and titanite, and these are more susceptible to alteration and recrystallisation than zircon. As shown by Hammerli et al. (2014), disturbance and re-equilibration of LREE-rich phases during metamorphism hinders determination of accurate initial Nd isotope compositions. Ham-

merli et al. (2019) and Fisher et al. (2020) examined the Sm-Nd isotope systematics of Eoarchean Itsaq and Acasta gneisses, respectively. These studies showed that Nd-rich accessory phases in these rocks were reset with respect to zircon U-Pb and bulk rock Sm-Nd isotopes during later tectono-thermal events and are out of equilibrium with their bulk rock compositions. Hammerli et al. (2019) further showed how positive $\varepsilon_{\text{Nd}(i)}$ in early Archean rocks can be an artifact of these secondary processes. Many Eo-to-Mesoarchean rocks are highly metamorphosed, which brings into question the assumption that Sm-Nd isotope compositions of early Earth samples are primary magmatic features. Additionally, complex histories of most Archean rocks make determination of magmatic protolith ages ambiguous (e.g., Whitehouse et al., 1999), further complicating retrieval of primary isotope compositions.

Although behavior of REE-rich accessory phases may be responsible for Sm-Nd mobility in some rocks, these minerals may also provide a means to identify samples in which the Sm-Nd isotope system has remained closed. Many REE-rich phases, such as monazite, titanite, and apatite, can also be dated using the U-Pb system (e.g., Amelin, 2009; Fisher et al., 2020). Thus, similar to coupled U-Pb age and Hf isotope information in zircon, these datable REE-rich phases can be used to place their Nd isotope compositions in a firm U-Pb chronological framework. In addition, the Sm-Nd isotope composition of these phases can be evaluated in the context of their corresponding whole rock sample to determine if the system has remained closed since crystallization at the bulk rock scale.

To better understand behavior of Sm-Nd isotope systematics in REE-rich accessory minerals in ancient rocks, this study focuses on well-preserved Paleoproterozoic granitic rocks of the Pilbara Craton of Western Australia (Fig. 1). Unlike many Eo-to-Mesoarchean localities, these samples largely escaped post-emplacement high-grade metamorphism (Van Kranendonk et al., 2002). We examine Lu-Hf isotope systematics by analysis of purified bulk rock solutions by MC-ICPMS and zircon by laser ablation (LA)-MC-ICPMS. We also determine Sm-Nd isotope compositions of purified bulk rock solutions in these samples, along with LA-MC-ICPMS analyses of titanite and apatite. We simultaneously measure U-Pb ages of zircon, titanite, and apatite in-situ using the Laser Ablation Split Stream (LASS) method to link age and isotope compositions.

This dataset demonstrates that Sm-Nd isotope systematics in these rocks and their accessory minerals preserve primary initial Nd isotope compositions. These relatively undeformed granitic rocks have initial Hf and Nd isotope compositions between 3.5–3.3 Ga that are chondritic (to slightly supra-chondritic) for both systems. The coupling of Hf and Nd isotopes in the Pilbara Paleoproterozoic granites demonstrates that mantle with a chondritic composition persisted beneath the Pilbara Craton until at least 3.3 Ga.

2. Background

2.1. The Pilbara Craton

The Pilbara Craton of Western Australia is one of the best-preserved examples of Paleo-to-Mesoarchean crust on Earth. It is characterized by a dome-and-keel granite-greenstone architecture, most conspicuously exposed in the East Pilbara Terrane (EPT) in the northeastern part of the craton. The eleven domes are large (~ 70 km across) ovoid granitic batholiths, surrounded by curvilinear greenschist-to-amphibolite facies greenstone belts. The early igneous record in the Pilbara Craton is represented by the ~ 3.59 Ga gabbroic rocks in the Shaw Granitic Complex (Petersson et al., 2019) and the 3.60–3.58 Ga zircon U-Pb ages of tonalite gneiss enclaves in a ~ 3.33 Ga monzogranite from the Warrawagine complex (Nelson, 1999; Kemp et al., 2015).

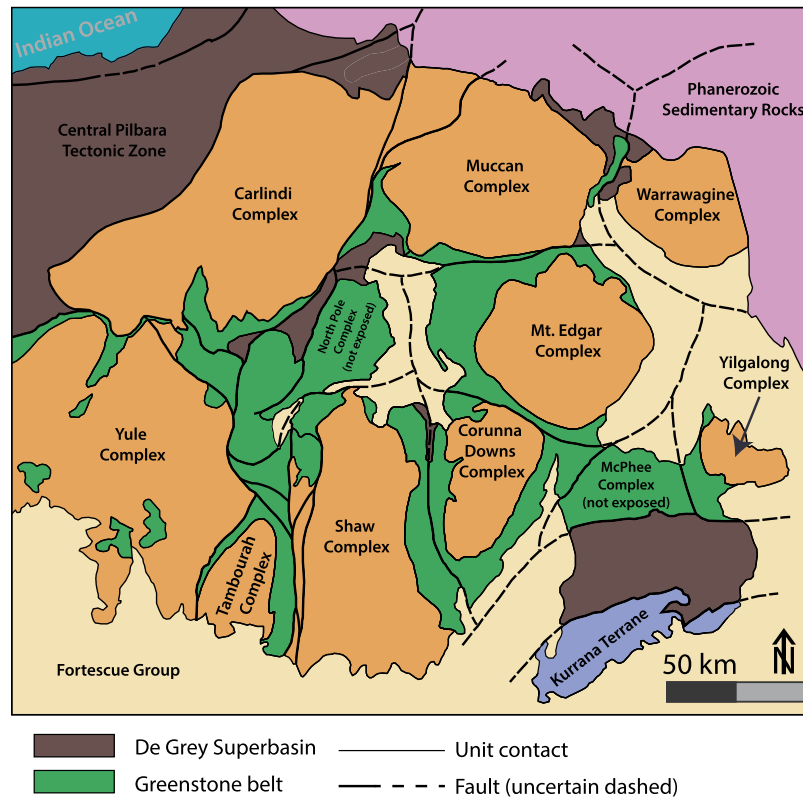


Fig. 1. Generalized geologic map of the East Pilbara Craton (after Hickman, 2012) showing the eleven exposed granitic complexes.

2.2. The igneous evolution of the Mt. Edgar Granitic Complex

This study focuses on the Mt. Edgar Granitic Complex (MEGC), which is arguably the best exposed, most accessible, and thus best studied granitic complex in the East Pilbara Terrane. The MEGC is comprised of multiple granitic intrusions, emplaced between 3.48 and 2.83 Ga (Hickman, 2012). The earlier igneous suites (3.49 to 3.41 Ga) are largely TTG gneisses; younger Paleoproterozoic suites (3.32 to 3.22 Ga) are less foliated and are more compositionally evolved. The youngest rocks in the MEGC were emplaced in the Neoproterozoic (2.85 and 2.83 Ga) and have compositions including monzogranite and syenogranite.

Gardiner et al. (2017) reported Hf and Nd isotope data on previously dated MEGC rocks. According to this study, the MEGC zircons (3.49 to 3.27 Ga) have a large range of Hf isotope compositions that span 6–8 $\epsilon_{\text{Hf}(i)}$ units, within a single sample; mean $\epsilon_{\text{Hf}(i)}$ values are chondritic to positive (0 to +3). Bulk rock $\epsilon_{\text{Nd}(i)}$ values are 0 to +1 for the same samples. The younger MEGC suites have slightly negative mean $\epsilon_{\text{Hf}(i)}$ (–2 to 0) in zircon. The Neoproterozoic rocks have much less radiogenic isotope compositions (zircon $\epsilon_{\text{Hf}(i)}$ of –2.7; whole rock $\epsilon_{\text{Nd}(i)}$ of –7.1).

Gardiner et al. (2017) argued the apparent trend of MEGC granitic rocks towards less radiogenic Hf and Nd isotope compositions suggests that the younger Paleoproterozoic rocks represent reworked ~3.63 Ga crust, with only a minor juvenile component. Recent work by Petersson et al. (2020), however, is at odds with this model. Their Pilbara-wide study reported zircon Hf and O isotope compositions in a set of 3.59–3.31 Ga granitic samples that are homogeneous and broadly chondritic, with $\epsilon_{\text{Hf}(i)} \sim 0$ and $\delta^{18}\text{O} = +6$, over ~300 million years of igneous activity. Petersson et al. (2020) suggested that continuous juvenile magmatism from a chondritic mantle source best explains the Paleoproterozoic evolution of the East Pilbara Terrane.

3. Methods and samples

Samples were selected from multiple igneous supersuites in the MEGC spanning most of its igneous history (Table 1). Sample and petrographic descriptions of all samples are provided in supplementary file 1. Analytical methods used in this study have been described elsewhere (Goudie et al., 2014; Fisher et al., 2014; Gaschnig et al., 2011; Johnson et al., 2018) and are also described in supplementary file 2. The U–Pb, Hf, and Nd isotope values of mineral standards used in this study are reported in Appendix 1.

4. Results

4.1. Bulk rock major and trace element chemistry

All samples plot within the TTG compositional fields defined on quartz–alkali–plagioclase and anorthite–albite–orthoclase ternary diagrams defined by Barker (1979) (Appendix 2; Supplementary file 3). The chondrite-normalized REE compositions of these samples all show similar LREE enrichment and HREE depletion patterns with negligible Eu anomalies.

4.2. U–Pb and Hf isotopes in zircon

The U–Pb results are given in Appendix 2. Textural descriptions and BSE images of zircon are given in supplementary file 4. The U–Pb data show varying degrees of discordance, with a maximum of 35% (AME18-039), but overall is minor (Fig. 2). Regressions yield imprecise lower intercepts near 0 Ma and well-constrained Paleoproterozoic upper intercept dates that range from 3469 ± 12 Ma to 3287 ± 10 and that agree well with the mean $^{207}\text{Pb}/^{206}\text{Pb}$ dates of the analyses (3467 ± 8 to 3288 ± 5 Ma, 2SE).

The corresponding zircon Lu–Hf isotope data are characterized by low $^{176}\text{Lu}/^{177}\text{Hf}$ (0.0003 to 0.0029) and near chondritic ini-

Table 1
Summary information for the samples included in this study.

Sample	Unit	Latitude/Longitude	Outcrop description
AME18-039	Campbell granodiorite	-21.171595, 119.790342	Medium-to-coarse grained weakly foliated biotite granodiorite
AME18-043	Zulu granodiorite	-21.217753, 120.324045	Medium grained weakly foliated biotite granodiorite to tonalite
AME18-068	Underwood gneiss	-21.331401, 119.920527	Coarse grained banded biotite tonalite gneiss
AME18-116	Kennell granodiorite	-21.319744, 120.014133	Medium grained weakly foliated biotite granodiorite with local mafic enclaves
AME18-134	Coppin Gap granodiorite	-20.952094, 120.142252	Coarse grained weakly foliated biotite-hornblende granodiorite with local mafic enclaves
AME18-167	Joorina granodiorite	-21.254860, 120.000028	Medium-to-coarse grained weakly foliated biotite granodiorite

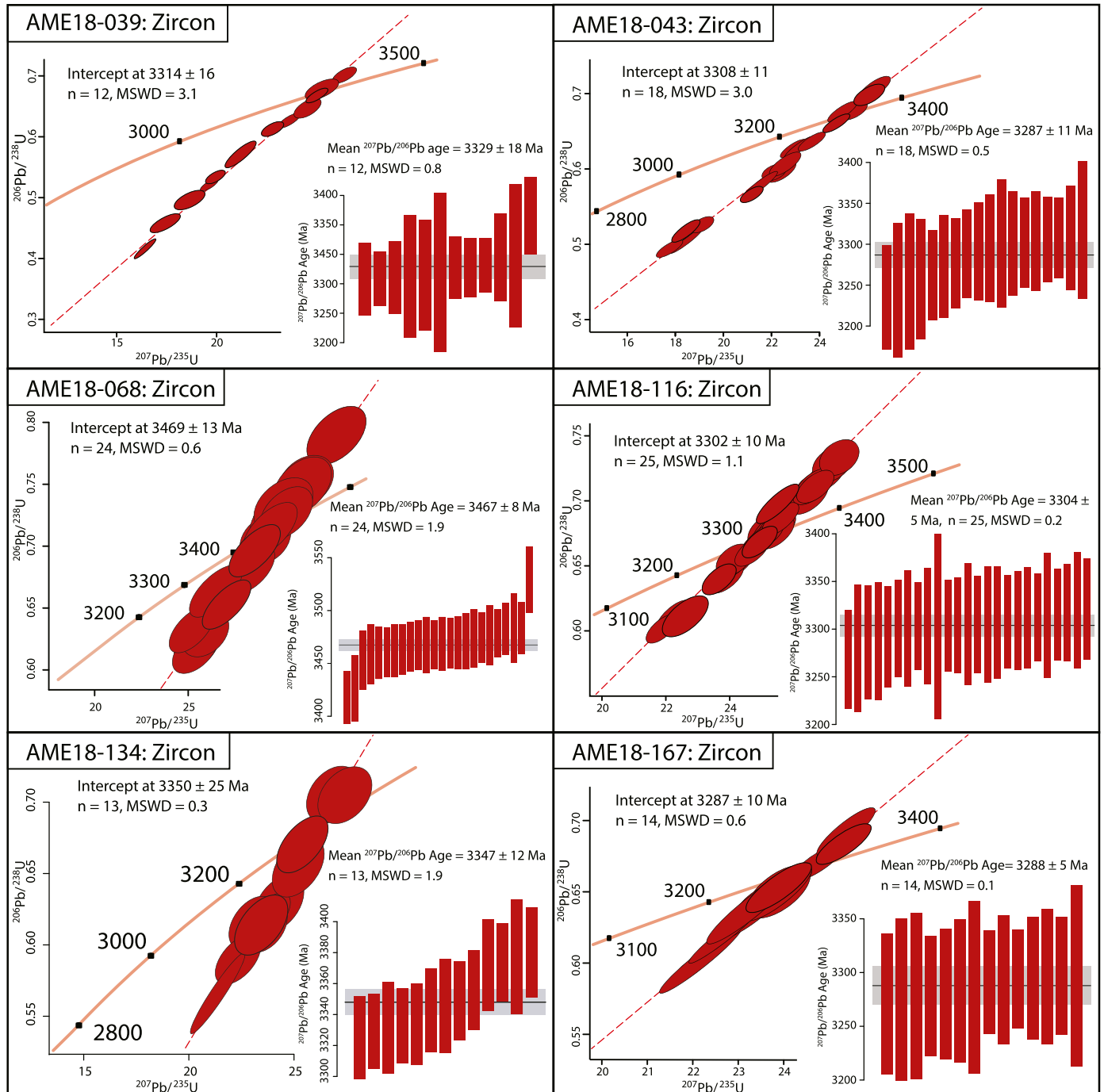


Fig. 2. Concordia plots of zircon LASS U-Pb data for six granitic rocks collected in the MEGC. The insets show individual $^{207}\text{Pb}/^{206}\text{Pb}$ dates and the associated weighted mean dates. All uncertainties are reported at 2SE.

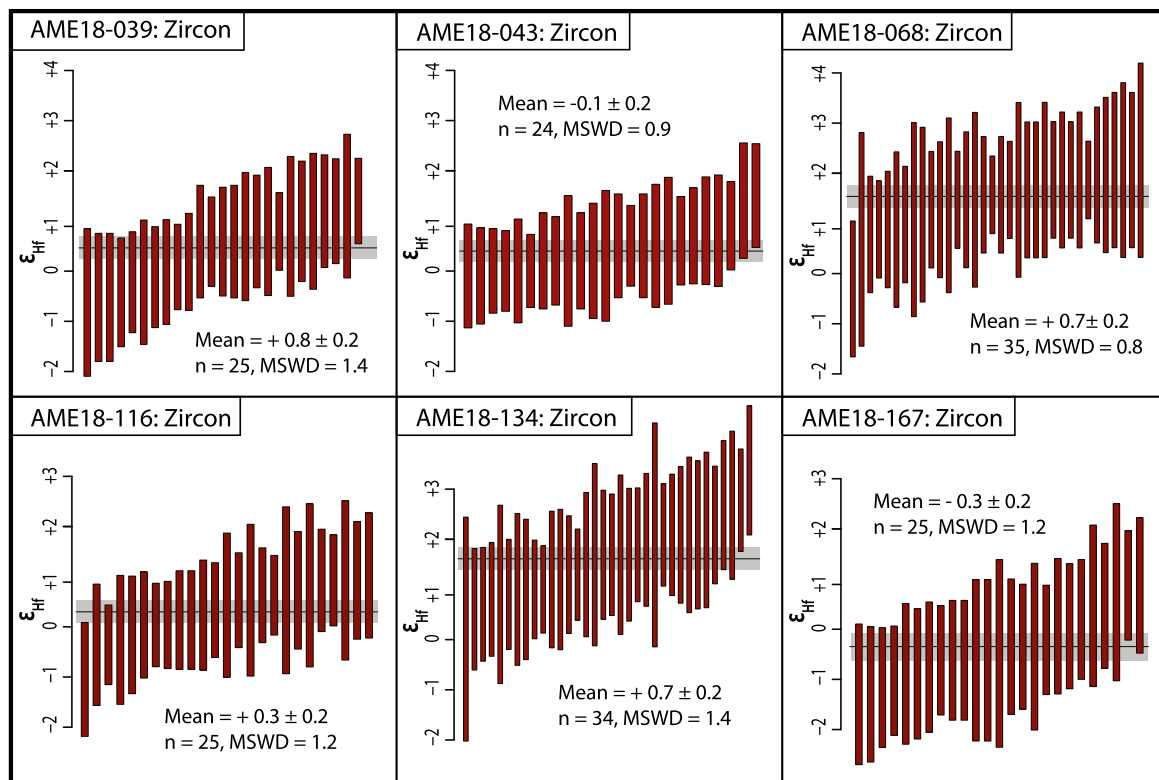


Fig. 3. Initial ϵ_{Hf} compositions of zircons in six granitic samples from the MEGC. Initial Hf isotope compositions are calculated at the mean $^{207}\text{Pb}/^{206}\text{Pb}$ ages reported in Fig. 2. All uncertainties are reported at 2SE.

tial $^{176}\text{Hf}/^{177}\text{Hf}$ (0.280503 to 0.280688) at the sample's respective mean $^{207}\text{Pb}/^{206}\text{Pb}$ date (Fig. 3). The individual zircon $\epsilon_{\text{Hf}(i)}$ determinations within each sample overlap within error and define homogeneous populations with low MSWD values. The mean $\epsilon_{\text{Hf}(i)}$ of samples in this study are close to chondritic ($+0.8 \pm 0.2$ at 3329 Ma to -0.3 ± 0.2 at 3288 Ma, 2SE; Fig. 3).

Initial ϵ_{Hf} values were also calculated from bulk rock Lu-Hf isotope data, using their corresponding zircon $^{207}\text{Pb}/^{206}\text{Pb}$ ages. The $\epsilon_{\text{Hf}(i)}$ values of 4 samples are near chondritic, being in accord with their respective zircon values. Sample AME18-134 is slightly more radiogenic, with $\epsilon_{\text{Hf}(i)}$ of +1.3. Multiple whole-rock Lu-Hf analyses of sample AME18-068 did not reproduce and had significant interferences of ^{176}Yb and ^{176}Lu on measurement of ^{176}Hf , and therefore we could not determine a value (Table 2).

4.3. U-Pb dating in titanite, and Sm-Nd isotopes in titanite and apatite

4.3.1. Titanite and apatite U-Pb dating

Titanite from the six samples were analyzed for U-Pb age and Nd isotope composition by LASS (Fig. 4; Appendix 2). Textural descriptions of titanite and BSE images are given in supplementary file 5. The U-Pb data from all samples overlap concordia, or nearly so, but the spread along concordia does not allow precise regression of intercepts or determination of concordia ages. The titanite in some samples have large ranges in $^{207}\text{Pb}/^{206}\text{Pb}$ dates (~ 150 Ma in the case of AME18-039 and AME18-068) but the range is more modest in others (~ 50 Ma for AME18-116 and AME18-134). As there is good evidence for significant common-Pb components (^{204}Pb) in titanite, we report the concordia ages of the analyses with the highest $^{206}\text{Pb}/^{204}\text{Pb}$ (i.e., lowest ^{204}Pb) as the maximum titanite U-Pb age of these samples. These ages range from 3491 ± 28 Ma (MSWD = 10) to 3285 ± 12 (MSWD = 2.1).

The U-Pb systematics of apatite in these samples are more ambiguous and do not provide useable age constraints due to high common Pb contents and the effects of ancient Pb-loss. These data

are reported in Appendix 2 and plotted in supplementary file 6. Textural descriptions of apatite and BSE images are given in supplementary file 7.

4.3.2. Titanite, apatite, and bulk-rock Sm-Nd isotopes

Titanite and apatite LASS Sm-Nd isotope data are given in Appendix 2. Apatite typically has lower $^{147}\text{Sm}/^{144}\text{Nd}$ than titanite (0.10–0.36 vs. 0.13–0.56) but with considerable overlap (Fig. 5). Titanite and apatite Sm-Nd data in all samples form coherent arrays on isochron diagrams that yield reasonably precise dates and initial $^{143}\text{Nd}/^{144}\text{Nd}$ values. Allanite is present in all of these samples as the mineral with the lowest Sm/Nd. We analyzed Nd isotopes in allanite, but due to metamictization and replacement by epidote these data are complicated and not considered further. Titanite-apatite-bulk rock isochron dates range from 3514 ± 99 Ma to 3147 ± 112 Ma, which generally agree with the U-Pb zircon and titanite dates, albeit with greater uncertainties. The initial ϵ_{Nd} of these samples, determined from the collective titanite-apatite-bulk rock isochrons, are broadly chondritic and range from -0.9 ± 0.5 to $+1.3 \pm 2.5$. These ages and intercept ϵ_{Nd} values also agree well with the titanite-apatite isochrons plotted in supplementary figure 1, where the bulk rock Sm-Nd values are excluded from the regression.

The mean titanite $\epsilon_{\text{Nd}(i)}$ range from $+2.0 \pm 2.0$ at 3469 Ma to -1.0 ± 0.3 at 3304 Ma, while mean apatite $\epsilon_{\text{Nd}(i)}$ range from -0.6 ± 2.1 at 3469 Ma to $+0.9 \pm 0.3$ at 3329 Ma, both in good agreement with initial Nd determined by the regression, giving further credence to the accuracy of the in-situ Sm-Nd method (Fig. 5 insets). The $\epsilon_{\text{Nd}(i)}$ of the bulk-rock samples range from $+0.1$ to $+1.2$ (calculated at the zircon $^{207}\text{Pb}/^{206}\text{Pb}$ age) and agree with $\epsilon_{\text{Nd}(i)}$ regressed from isochrons in Fig. 5, as well as the mean of LASS $\epsilon_{\text{Nd}(i)}$ calculated for the individual accessory phase using the zircon U-Pb age. These relationships are highlighted in supplementary Fig. 2.

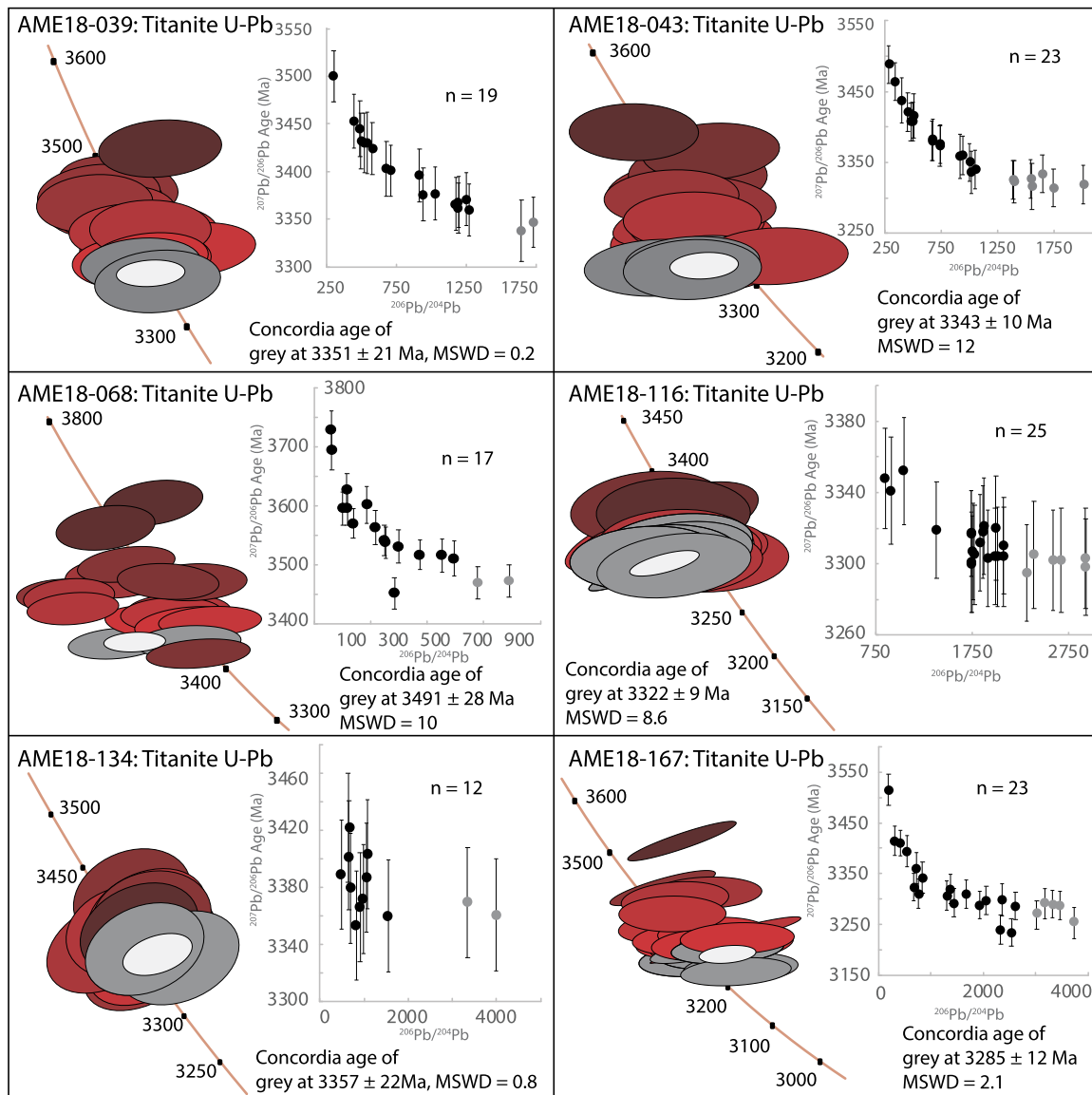


Fig. 4. Concordia plots of titanite LASS U-Pb data for six samples. Ellipses are shaded according to $^{206}\text{Pb}/^{204}\text{Pb}$ value – with darker colors indicating relatively lower values. We plot the $^{206}\text{Pb}/^{204}\text{Pb}$ ratios against the $^{207}\text{Pb}/^{206}\text{Pb}$ dates of each analysis to monitor the common-Pb component. In every sample, there is a negative correlation between the $^{207}\text{Pb}/^{206}\text{Pb}$ dates and $^{206}\text{Pb}/^{204}\text{Pb}$ values of the analyses, indicating higher ^{204}Pb with older apparent $^{207}\text{Pb}/^{206}\text{Pb}$ dates. In all cases, analyses with relatively lower $^{206}\text{Pb}/^{204}\text{Pb}$ values plot higher on Concordia, toward older apparent ages. The white ellipse on each diagram represents the concordia age from analyses with the least common Pb, shaded in grey. The grey data points on the inset represent the grey ellipses on concordia. All uncertainties are reported at 2SE. (To view the colors in the figure(s), the reader is referred to the web version of this article.)

5. Discussion

5.1. Assessing U-Pb geochronology and Hf isotopes

5.1.1. U-Pb geochronology

The simple zircon U-Pb systematics of the 6 samples in this study are in keeping with well-preserved magmatic microstructures of these crystals (Fig. 2; supplementary file 4). There is no evidence for metamorphic overgrowths, inheritance, or ancient Pb-loss events in the zircon U-Pb data and we interpret these dates as representing igneous crystallization ages. Zircon U-Pb ages range from 3.47 Ga to 3.28 Ga and agree with those previously published for these units (Williams and Collins, 1990; Nelson, 1999; Williams and Bagas, 2007; Hickman and Van Kranendonk, 2012).

Interpreting titanite U-Pb dates for these samples is more complicated due to variable common Pb content. As described above, we estimate titanite crystallization ages using analyses with the

highest measured $^{206}\text{Pb}/^{204}\text{Pb}$. These ages range from 3.49 to 3.28 Ga and are in broad agreement with zircon magmatic ages (Fig. 6) and are thus regarded as recording timing of igneous crystallization. This interpretation is consistent with petrographic evidence, as the titanite grains are euhedral-to-subhedral and have oscillatory zoning (Supplementary file 5).

5.1.2. Hf isotopes

The zircon Hf isotope compositions have consistent $\varepsilon_{\text{Hf}(t)}$ both within an individual sample (MSWD values ~ 1) and between samples ($\varepsilon_{\text{Hf}(t)} = -0.3$ to $\varepsilon_{\text{Hf}(t)} = +0.8$; Fig. 3). These values indicate the zircon Hf isotope data are homogeneous and do not show evidence of multiple components or open-system behavior. The near-chondritic initial Hf isotope compositions indicate that the parental magmas were derived from a reservoir that was broadly chondritic over the 200 Ma age range (3.47 to 3.28 Ga) of the studied granites.

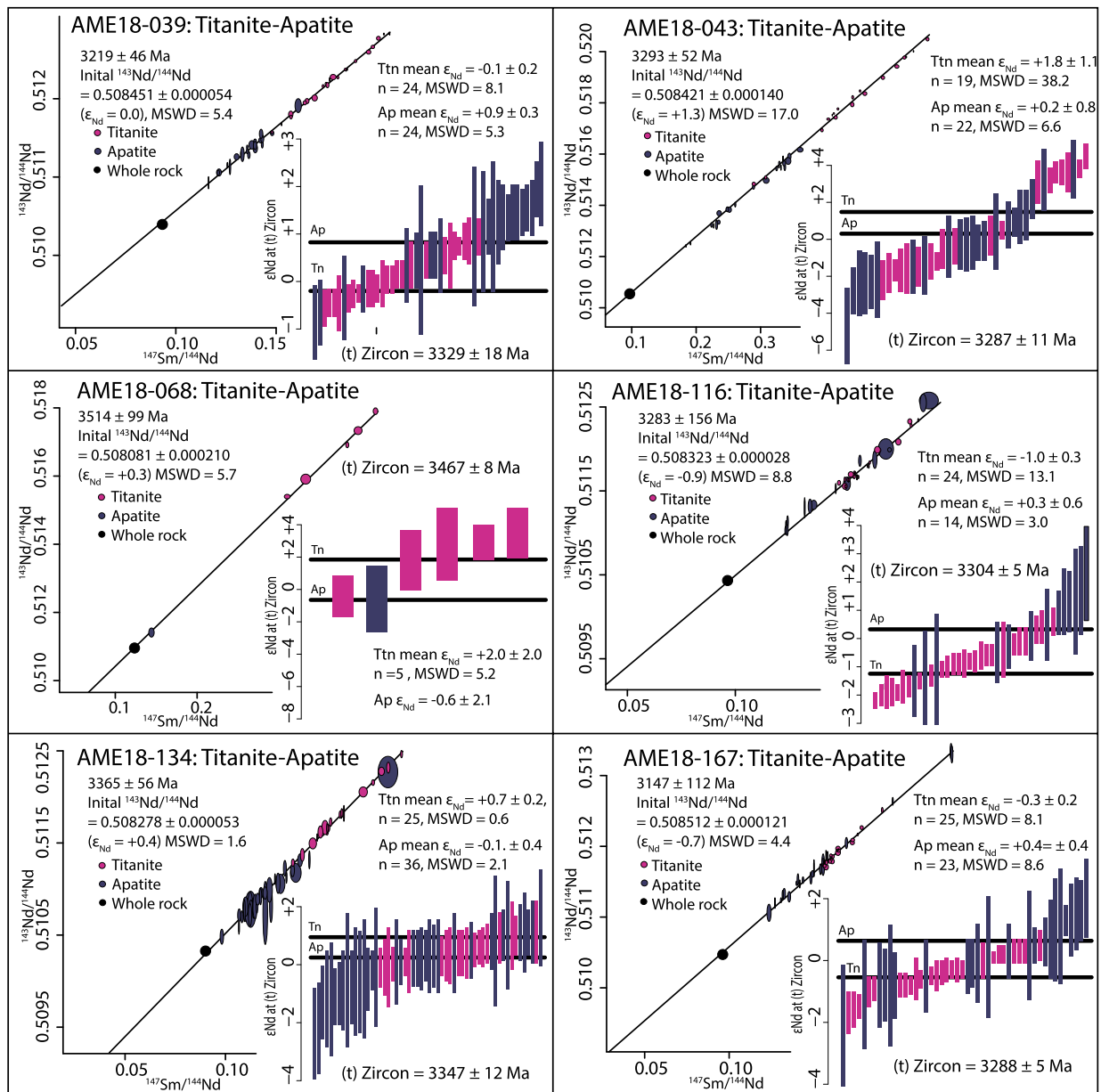


Fig. 5. Titanite and apatite Sm-Nd isotope compositions determined by LASS. Titanite, apatite, and bulk rock Sm-Nd compositions are plotted on isochron diagrams for each sample. Plots adjacent to isochrons show the mean ϵ_{Nd} of the titanite and apatite analyses, determined at the sample's respective zircon $^{207}\text{Pb}/^{206}\text{Pb}$ age reported in Fig. 2. The black bars on the plots indicate the mean titanite and apatite $\epsilon_{\text{Nd}(t)}$ values. All data are reported at 2SE uncertainty. These data were filtered to only include analyses with in-run uncertainties less than 2.5 epsilon units. All uncertainties are reported at 2SE.

Several other recent studies have reported zircon Hf isotope data for Paleoproterozoic granitic rocks in the EPT. Gardiner et al. (2017) reported initial Hf isotope values for previously dated zircons in the MEGC with $^{207}\text{Pb}/^{206}\text{Pb}$ ages ranging between 3.44 to 3.22 Ga. These authors used the measured $^{207}\text{Pb}/^{206}\text{Pb}$ date for each zircon to calculate the grain's initial Hf isotope ratio and then interpret each Hf isotope measurement as having specific meaning rather than using the mean Hf isotope value calculated at the interpreted magmatic crystallization age. Using this approach, they reported a large range of $\epsilon_{\text{Hf}(t)}$ in zircon, between +3.9 (at 3.32 Ga) and -5.6 (at 3.25 Ga), trending towards negative values with time. They interpreted this to indicate inherited >3.60 Ga crustal components in these rocks.

A contrasting approach was taken by Petersson et al. (2019, 2020), who report U-Pb ages, and Hf and O isotope values, of zircon in rocks from the Warravagine, Muccan, Carlindi, and Shaw

granitic complexes. In these studies, zircon Hf isotope compositions showed a limited spread for individual samples, and mean $\epsilon_{\text{Hf}(t)}$ values were therefore computed at the magmatic crystallization age, as determined by U-Pb isotopes (e.g., Vervoort and Kemp, 2016). Petersson et al. (2019) characterized the oldest igneous rocks yet found in the Pilbara, at 3.59 Ga, with $\epsilon_{\text{Hf}(t)}$ of -0.4 to -0.2 and mantle-like zircon $\delta^{18}\text{O}$ (+5.3 to +5.9). Subsequently, Petersson et al. (2020) found that broadly chondritic mean $\epsilon_{\text{Hf}(t)}$ values, along with mantle-like to slightly elevated $\delta^{18}\text{O}$, characterized the 3.58 Ga to 3.31 Ga granitic rocks in the EPT. A homogeneous and approximately chondritic mean zircon $\epsilon_{\text{Hf}(t)}$ ($\sim +0.6$) was also established by Kemp et al. (2017) for the 3.47 Ga Owen's Gully Diorite of the MEGC, by both solution and laser ablation mode analysis.

Our new Hf isotope data agree with the values reported by Petersson et al. (2019, 2020) and show no evidence for either

Table 2
Bulk rock Lu-Hf and Sm-Nd isotope compositions of the Pilbara Granites.

Sample	Age (Ga)	Lu (ppm)	Hf (ppm)	Sm (ppm)	Nd (ppm)	$^{176}\text{Lu}/^{177}\text{Hf}$	$^{176}\text{Lu}/^{177}\text{Hf}$ ±	$^{143}\text{Nd}/^{144}\text{Nd}$	$^{147}\text{Sm}/^{144}\text{Nd}$ ±	$\epsilon\text{Nd}_{(0)}$	$\epsilon\text{Nd}_{(i)}$	$\epsilon\text{Hf}_{(0)}$	$\epsilon\text{Hf}_{(i)}$
AME18-039	3.33	0.176	4.054	4.940	32.020	0.281086	3	0.510395	6	0.0933	+0.3	-61.4	+0.6
AME18-043	3.31	0.103	3.148	3.120	19.490	0.280957	10	0.510520	7	0.0969	+1.1	-64.6	+0.6
AME18-068	3.47	-	-	2.790	15.380	-	-	0.510699	6	0.1097	1.0	-	-
AME18-116	3.30	0.139	4.606	4.010	25.310	0.280931	2	0.510449	6	0.0957	+0.1	-65.5	+0.4
AME18-134	3.35	0.120	3.269	3.430	23.240	0.280992	3	0.510325	9	0.0892	+1.2	-63.4	+1.3
AME18-167	3.29	0.246	4.862	8.050	50.560	0.281115	2	0.510471	6	0.0962	+0.2	-59.1	+0.1

We calculated the Initial Nd isotope values of these samples using the CHUR parameters of Bouvier et al. (2008), $^{143}\text{Nd}/^{144}\text{Nd} = 0.512630$ and $^{147}\text{Sm}/^{144}\text{Nd} = 0.1960$, and the ^{147}Sm decay constant of Lugmair and Marti (1978) of $6.54 \times 10^{-12} \text{ y}^{-1}$. Initial Hf isotope values were calculated using the CHUR parameters of Bouvier et al. (2008), $^{176}\text{Lu}/^{177}\text{Hf} = 0.282785$ and $^{176}\text{Lu}/^{177}\text{Hf} = 0.0336$, and the ^{176}Lu decay constant of Söderlund et al. (2004) of $1.867 \times 10^{-11} \text{ y}^{-1}$. All results are presented with 2SE precision.

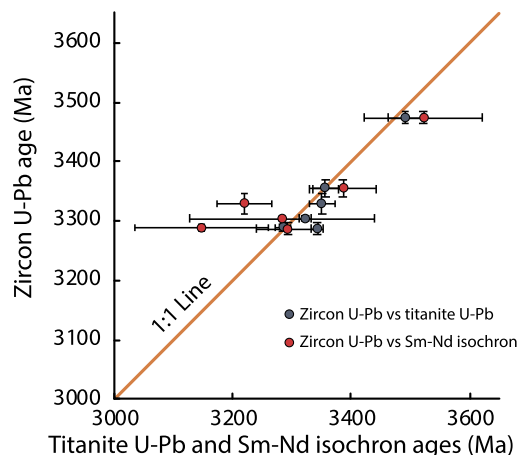


Fig. 6. Comparison between the zircon U-Pb, titanite U-Pb, and Sm-Nd isochron dates of the 6 samples in this study. All uncertainties are reported at 2SE.

crustal inheritance or contribution from a depleted mantle reservoir. Rather, the consistently chondritic initial Hf isotope values suggest these rocks were derived from a juvenile precursor with a chondritic Hf isotope composition.

5.2. Sm-Nd geochronology and Nd isotopes

Samarium-neodymium isochrons are useful for interpreting both ages and initial Nd isotope compositions of rocks. Our approach assesses integrity of the Sm-Nd isotope system in these rocks and tests whether they have remained closed since their formation. While lack of large Sm/Nd fractionation results in rather imprecise age and initial ϵNd determinations, the in-situ LA-MC-ICPMS method is sufficiently precise to resolve disequilibria on the scale of a few epsilon units.

The Sm-Nd isochron dates for the six samples in this study range from 3.51 to 3.15 Ga and are in general agreement with zircon and titanite U-Pb dates for each sample (Fig. 6), although 2 of the samples (AME18-167 and AME18-039) have younger Sm-Nd isochron ages. This demonstrates that the Sm-Nd isotope system has remained closed in these rocks since their formation and that these minerals are primary and crystallized together with zircon.

Similarly, as expected for a closed system, the $\epsilon\text{Nd}_{(i)}$ of titanite and apatite are identical, and the different approaches used to determine initial Nd isotope compositions all converge on the same, broadly chondritic values, as follows: 1) the $\epsilon\text{Nd}_{(i)}$ values determined from the intercept on the titanite-apatite-bulk rock isochrons range from -0.9 to $+1.3$ (Fig. 5); 2) mean $\epsilon\text{Nd}_{(i)}$ values determined for each sample from the individual titanite and apatite analyses (Fig. 5) range from -0.6 to $+0.9$ (apatite) and from -1.0 to $+2.0$ (titanite); and 3) the $\epsilon\text{Nd}_{(i)}$ values determined from the bulk rock composition at their crystallization ages range from $+0.1$ to $+1.2$ (Table 2). In total, the Sm-Nd isotope compositions of these rocks and constituent minerals further indicate these rocks are closed systems and retain their original Nd isotope compositions.

Nd isotopes have been reported in previous studies for the supracrustal rocks and the granitic suites in the East Pilbara Terrane. The $\epsilon\text{Nd}_{(i)}$ values range from -0.3 ± 0.2 , for a 3.45 Ga Warrawoona group basalt, to as high as $+4.0$, in the case of the 3.47 Ga Mt. Ada basalt (Jahn et al., 1981; Gruau et al., 1987; McCulloch, 1987; Arndt et al., 2001; Smithies et al., 2009). The $\epsilon\text{Nd}_{(i)}$ of granitic rocks in the East Pilbara Terrane range from -1.3 ± 0.6 , in the 3.47 Ga Chocolate Hill suite of the Shaw Granitic Complex, to $+2.1 \pm 0.4$ for 3.43 Ga granites in the Corunna Downs Granitic Complex (McCulloch, 1987; Bickle et al., 1993; Smithies et al., 2007;

Nelson, 1999; Gardiner et al., 2017). The positive $\varepsilon_{\text{Nd}(i)}$ have generally been taken to represent a depleted mantle component in these rocks (e.g., Gruau et al., 1987), and negative values the assimilation of older crustal material (e.g., Arndt et al., 2001).

Compared with our results, previous studies report a wider range in $\varepsilon_{\text{Nd}(i)}$, with both more highly positive and negative values. Although this could be interpreted as reflecting a heterogeneous source, there may be other factors contributing to a more varied data set such as open-system Sm-Nd behavior or inaccuracy in calculation of $\varepsilon_{\text{Nd}(i)}$ due to assignment of inaccurate crystallization ages. In the case of the mafic compositions, even though they lack firm zircon age constraints, this is not likely to significantly contribute to inaccurate initial Nd determinations. This is because these lithologies have Sm/Nd ratios similar to the CHUR, and thus their calculated initial ε_{Nd} compositions do not appreciably change over the time span of any reasonable age inaccuracy. More significant is the potential for open-system behavior in the mafic-ultramafic compositions as discussed below.

5.3. Evaluating the Nd isotope record

Neodymium and Hf isotopes provide important tools for tracking rates and processes by which the Earth's crust was extracted from the mantle over geologic time (e.g., DePaolo, 1981; McCulloch and Bennett, 1994; Vervoort and Blichert-Toft, 1999). Increasingly, however, it is becoming apparent that geologic complexities have resulted in heterogeneities in the isotope record—particularly for the early Earth—that do not reflect the rock's primary isotope composition. Therefore, an approach is needed that allows for careful evaluation of the integrity of Nd and Hf isotope records.

For Hf isotope data from zircon-bearing magmatic rocks, this can be straightforward: determine igneous crystallization ages from collective U-Pb systematics in zircon population(s) and use these ages to determine initial zircon Hf isotope compositions. Complexities in either age or Hf isotope compositions due to factors such as ancient Pb loss, inheritance, overgrowths, mixing of components, and open-system behavior can be assessed through collective U-Pb and Lu-Hf isotope data from the zircon population. Doing this confidently in absence of zircon or other datable Hf-rich phases (e.g., as for mafic and ultramafic rocks, or with stand-alone zircon analyses (e.g., in detrital zircon studies)), however, is not straightforward due to potential age ambiguities (e.g., Vervoort and Kemp, 2016).

Utilizing datable REE-rich accessory phases, as done here, provides a method—similar to what is employed for the Hf isotope system—to assess closed-system behavior for the Nd isotope system. In the present study, we are able to do this by integrating the U-Pb and Sm-Nd isotope system in titanite, apatite, and whole rock compositions: 1) titanite U-Pb dates are in agreement with the zircon U-Pb dates for each sample demonstrating that these phases were likely primary and formed at the same time as co-existing zircon; 2) titanite, apatite, and bulk rock compositions yield Sm-Nd isochron dates consistent with titanite and zircon U-Pb dates demonstrating that, within uncertainty, Sm-Nd records the same system closure in these rocks as U-Pb (Fig. 6); and 3) initial Nd isotope compositions determined for each sample from the titanite-apatite-bulk rock isochron, individual titanite and apatite analyses, and from the bulk rock analysis, yield consistent values and demonstrate that the Sm-Nd system has been closed in these rocks since their original formation and faithfully preserves the Nd isotope composition of the magma.

A fully closed Nd isotope system is not assured for all rocks in the Archean record—particularly for rocks subjected to higher metamorphic grades. A useful way to evaluate the Hf and Nd isotope compositions of samples is to examine how they plot with respect to the terrestrial Hf-Nd array (Fig. 7). The terrestrial array

is defined by the correlative Hf and Nd isotope compositions of crust and mantle materials, generally following the relationship $\varepsilon_{\text{Hf}} = 1.50 \varepsilon_{\text{Nd}} + 1.57$ for initial compositions (Vervoort et al., 2011). Shown in Fig. 7a is a plot of >3.6 Ga gneisses from SW Greenland for which there are zircon Hf and whole-rock Nd isotopes on the same sample. This diagram illustrates a notably narrower range in $\varepsilon_{\text{Hf}(i)}$ (~ -1 to $+3$) in contrast to a large variation in $\varepsilon_{\text{Nd}(i)}$ ($9 \varepsilon_{\text{Nd}}$ units, -4.5 to $+4.5$). Moreover, the expectation is for less variation in Nd than Hf because of the general behavior that characterizes the terrestrial array (i.e. $\varepsilon_{\text{Hf}} \sim 1.5 \times \varepsilon_{\text{Nd}}$).

Several studies have demonstrated open Sm-Nd isotope system behavior: in the Eo-Paleoarchean rocks from southern West Greenland (Amelin, 2009; Hammerli et al., 2019) and from the Acasta Gneiss complex in NWT, Canada (Fisher et al., 2020). In these cases, zircon U-Pb and Sm-Nd isotope systematics have been modified during later high-grade regional metamorphic events and demonstrate mobility of Sm and Nd due to the breakdown of less-stable LREE-rich accessory minerals accompanying tectonothermal events. The Lu-Hf systems in these studies, however, were unaffected, as Hf is largely anchored in zircon. The Hf and Nd isotope data from the present study are shown as red boxes on Fig. 7. In contrast to the Hf and Nd literature values of the data shown in Fig. 7a, the Pilbara data presented here have a narrow range of both Hf and Nd isotope compositions and plot within the terrestrial array with the expected Hf-Nd relationship for closed systems.

A second, related point—namely, open-system behavior in the Lu-Hf isotope system—is illustrated in Fig. 7b which plots whole-rock Lu-Hf and Sm-Nd isotope records for >3.6 Ga Greenland rocks. The granitic gneisses have a similar range in Hf isotopes as do the zircon data, but mafic and ultramafic samples have dramatically more variability, particularly toward very high ε_{Hf} values (up to $\varepsilon_{\text{Hf}} = +12.9$), that is not generally reflected in the Nd isotope data. It has been argued that the high ε_{Hf} values in these rocks demonstrate existence of highly depleted mantle reservoirs in the Hadean (Hoffmann et al., 2011). An alternative interpretation—and one that is more realistic in our opinion—is that these data result from open-system Lu-Hf behavior. Although Hf is generally immobile in felsic compositions, the same is not true in easily altered ultramafic compositions due to lack of robust phases to anchor Hf or Lu (Hoffmann and Wilson, 2017).

5.4. A highly heterogeneous Paleoproterozoic mantle in the Pilbara?

Several recent studies have reported heterogeneous initial Hf and Nd isotope compositions for the Paleoproterozoic rocks of the Pilbara Craton. Nebel et al. (2014) and Hasenstab et al. (2021) reported $\varepsilon_{\text{Hf}(i)}$ values as high as $+8.2$ for some Paleoproterozoic Pilbara supergroup basalts and komatiites. Both studies suggest these data indicate derivation of the basalt and komatiite samples from a melt-depleted mantle reservoir, possibly as old as ~ 4.2 Ga. In contrast, Tympel et al. (2021) examined a series of basalts and komatiites collected from drillcore in the Pilbara supergroup and determined these rocks have broadly chondritic to slightly positive $\varepsilon_{\text{Hf}(i)}$ and $\varepsilon_{\text{Nd}(i)}$ values. Similarly, Murphy et al. (2021) establish slightly positive $\varepsilon_{\text{Hf}(i)}$ and $\varepsilon_{\text{Nd}(i)}$ values for well-preserved ca. 3.47 Ga basaltic lavas of the Warrawoona Group. While Tympel et al. (2021) did find that some rocks have more variable initial radiogenic Hf and Nd ratios, these examples are restricted to the highly altered 3.48 Ga Dresser Formation, and were considered to be unreliable. As noted above, Gardiner et al. (2017) report LA-ICPMS zircon $\varepsilon_{\text{Hf}(i)}$ values scattering between $+4$ to -6 for several TTGs in the Mt. Edgar Granitic Complex. Gardiner et al. (2017) attribute these data to indicate derivation of the granitic magmas from a depleted mantle and an older enriched crustal reservoir, respectively—assuming that each measured value represents a stand-alone Hf isotope composition.

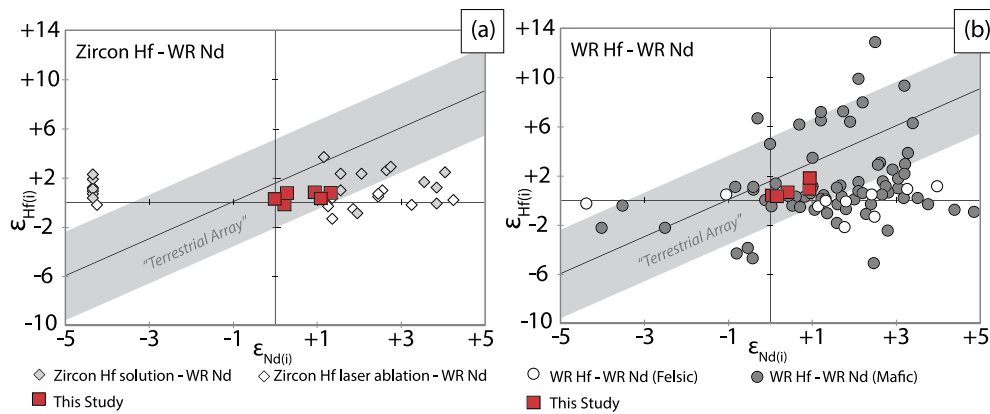


Fig. 7. Archean samples (> 3.5 Ga) from SW Greenland that have both Hf and Nd isotopes determined on the same sample. A) Zircon Hf (determined by solution or laser ablation) and whole-rock Nd. Note that the laser Hf isotope data have more uniform initial epsilon Hf values than the solution zircon analyses which were multigrain whole zircon analyses, some of which were done by TIMS (Vervoort et al., 1996). B) Bulk rock Hf and bulk rock Nd for felsic and mafic samples. Note that the felsic samples have relatively uniform initial epsilon Hf values, whereas the mafic samples are highly scattered, predominantly at higher positive epsilon values. Data are from Vervoort et al. (1996), Vervoort and Blichert-Toft (1999), Hoffmann et al. (2010; 2011), Rizo et al. (2011, 2012), and Kemp et al. (2019). Red boxes show the zircon Hf and WR Nd values of the Pilbara samples from this study. The terrestrial Hf-Nd array is from Vervoort et al. (2011).

In terms of Nd isotopes, Tessalina et al. (2010) report a Sm-Nd errorchron of 3.49 ± 0.10 Ga from a mixed collection of metakomatiites, metabasalts, barite and silicified carbonate from the Dresser Formation. The corresponding initial ϵ_{Nd} value of -3.3 was taken as evidence for an older crustal component in these rocks that separated from the mantle before 4.3 Ga.

If considered alone, the extremely radiogenic compositions of the basalts and komatiites would require that an ancient melt-depleted mantle existed beneath Pilbara Craton and that igneous rocks in the EPT were sourced from this reservoir, as argued by Nebel et al. (2014) and Hasenstab et al. (2021). These authors would also consider the variable-to-negative $\epsilon_{Hf(i)}$ and $\epsilon_{Nd(i)}$ values of the 3.5–3.4 Ga mafic rocks indicate significant assimilation of older crustal rocks into these melts. In total, these authors generally interpret these heterogeneous isotope data to argue that the Pilbara Craton has a long prehistory of crustal extraction, dating to as early as 4.2 Ga.

The highly variable Hf and Nd isotope data highlighted above are in stark contrast with the much more homogeneous—and broadly chondritic—Hf and Nd isotope data reported in the present study, and recently by Petersson et al. (2019, 2020) and Murphy et al. (2021). It is important to reconcile these conflicting datasets given the divergent implications for crust-mantle evolution that arise from these. We contend, as argued above, that the highly heterogeneous datasets are not an accurate representation of the Lu-Hf and Sm-Nd isotope composition of the magmatic protoliths to the Pilbara rocks.

Heterogeneities in the Hf and Nd isotope determinations can result from a number of sources: 1) open system behavior in the Lu-Hf or Sm-Nd isotope systems; 2) imprecision or inaccuracy in the zircon Hf isotope laser ablation measurements; or 3) how the measured zircon Hf isotope values are interpreted (individual analyses versus the mean of multiple measurements). These sources may have variously contributed to the heterogeneous isotope data reported for the Paleoproterozoic Pilbara rocks. In the first case, while it is true that mafic and ultramafic compositions represent a more direct sampling of the Pilbara mantle, such rocks—and especially komatiites and other ultramafic compositions—are readily altered. As Hf and the REE are contained in high temperature mafic silicates or in the mesostasis, open system Sm-Nd or Lu-Hf behavior is probable (e.g., Hammerli et al., 2019; Fisher et al., 2020). Indicative of alteration intensity are the large percentages of reported LOI (loss on ignition) evident in major element determinations for these rocks, even where relict igneous textures

are preserved (e.g., Murphy et al., 2021). In the second case, the accuracy and reproducibility of individual laser Hf isotope determinations can be compromised by a number of factors including poor precision, inadequate interference corrections, or mixtures of components during analysis (e.g., Fisher et al., 2014). Finally, spurious Hf heterogeneity can be produced by presenting each laser ablation Hf isotope analysis as representative of a single component paired with an individual U-Pb date, rather than using each analysis to contribute to the determination of a mean Hf isotope value at a magmatic age, in the same way as a zircon “age” is determined from multiple laser ablation U-Pb analyses (e.g., Vervoort and Kemp, 2016).

5.5. Implications for the origin of sialic material in the Pilbara Craton

The origin of sialic material in granite-greenstone terrains is of great interest because these compositions are fundamental to the growth and preservation of Earth’s earliest continents (Jacobsen and Wasserburg, 1979; de Witt et al., 1992). Geochemical and isotopic studies can provide constraints on these processes, including the melt source, the depths at which melts were generated, and timescales of magmatism and metamorphism. Our results show the granitic magmas in the MEGC were derived from a source with broadly chondritic Hf and Nd isotope compositions, over their ~ 200 Ma petrogenetic history. We interpret these isotope compositions as evidence that the granitic rocks were largely composed of juvenile material and, to a first order, represent new crustal additions from a chondritic mantle. As production of granitic magmas likely requires at least two stages of partial melting from their ultimate mantle source, Sm-Nd and Lu-Hf appreciably fractionate during this process. Because we see no significant evolution in the Nd and Hf isotope compositions over the timescale of magmatism in these Pilbara granites, this seems to indicate that the timescale of extraction from the mantle to generation of Archean granitic rocks was short, allowing little time for radiogenic ingrowth of ^{176}Hf or ^{143}Nd .

5.6. Towards a robust Hf-Nd isotope record of the early Earth

The global Nd and Hf isotope records through time have been used to model evolution of Earth’s crust and mantle geochemical reservoirs. To a first order, there is widespread agreement between Hf and Nd isotopes, particularly for rocks from the last half of Earth history: Rocks derived from what is interpreted to be the depleted mantle have positive $\epsilon_{Hf(i)}$ and $\epsilon_{Nd(i)}$ that increase through

time; conversely, crustal sources have negative $\epsilon_{\text{Hf}(i)}$ and $\epsilon_{\text{Nd}(i)}$ that become more negative with time and correspond to the antiquity of the crustal source. There is less agreement, however, between Hf and Nd isotopes in the Archean, particularly through the Eo-to-Paleoarchean.

One compilation of Hf and Nd isotope values through the Archean is shown in Fig. 8. For Hf isotopes we have focused on zircon in magmatic rocks for which a robust crystallization age exists. This compilation excludes detrital zircon data as well as zircon-free rocks such as most mafic and ultramafic compositions. The exception to this is the Jack Hills detrital zircon data set, included here because it covers the portion of Earth history for which there is no rock record.

The differences in the Hf and Nd isotope records are stark: there is large variation in ϵ_{Nd} —including the oldest samples—with a preponderance of positive ϵ_{Nd} for the Eoarchean (Fig. 8a). This scatter does not substantially lessen for whole-rock samples with zircon U-Pb ages (Fig. 8b). The zircon Hf isotope record from the best-preserved magmatic rocks (Fig. 8c) is strikingly different: 1) there is a broadly chondritic signature of the most radiogenic samples prior to ~ 3.5 Ga; 2) there are no unambiguously positive ϵ_{Hf} values prior to 3.5 Ga; 3) the oldest samples from Jack Hills detrital zircons and Acasta gneisses are characterized by negative ϵ_{Hf} that trend more negative with time; and 4) after ~ 3.5 Ga there are increasingly positive ϵ_{Hf} , although these plot well below a simple 4.5 Ga depleted mantle reference line for this segment of the Archean.

The Hf isotope records from both Jack Hills and Acasta are consistent with reworking of an early (Hadean) formed crust. In the case of Jack Hills, this has been interpreted as reworking of ~ 4.4 Ga mafic protocrust (e.g., Kemp et al., 2010). The oldest rocks in the Acasta Gneiss complex have the Hf isotope trend toward increasingly negative ϵ_{Hf} through time, interpreted as reworking of a >4.0 Ga crust (Bauer et al., 2017). Despite unambiguous signatures of early-formed crust in these datasets, there is no Hf isotope evidence in any of the pre-3.5 Ga samples for their derivation from a depleted mantle reservoir that had undergone long-term Lu-Hf depletion. Development of the depleted mantle reservoir, in the Hf isotope record, appears to start at 3.5–3.6 Ga when ϵ_{Hf} values begin to trend significantly above CHUR (Fig. 8c). This indicates that, prior to 3.5 Ga, not enough crust had been extracted to significantly change the Lu/Hf ratio of the mantle.

The Nd isotope record stands apart from its Hf isotope counterpart, in particular, with strongly positive ϵ_{Nd} values for pre-3.5 Ga samples (Fig. 8b). Collectively, Nd isotope data have been highlighted as providing evidence of differentiation of the silicate Earth into enriched crustal and depleted mantle reservoirs early in Earth's history (e.g., Armstrong, 1981; Bennett et al., 1993; Bowring and Housh, 1995; Caro et al., 2005; Bennett et al., 2007). It might be argued that the Hf and Nd isotope records shown here are not comparable in that the Lu-Hf dataset is weighted towards zircon-bearing intermediate to felsic rocks and the Sm-Nd dataset includes samples that do not contain zircon such as basalts and komatiites. This is refuted by Fig. 8b, which shows that the record of samples dated by zircon U-Pb (and, thus, largely excluding mafic-ultramafic rocks), is not appreciably different from the Nd isotope dataset as a whole; both panels 8a and 8b show large variability in epsilon values with a preponderance of positive values for pre-3.5 Ga samples.

When it can be demonstrated that isotope systems have been closed and samples are uncompromised, we argue that both systems yield consistent information and there is no Hf-Nd paradox. The Pilbara granitic Hf and Nd isotope data (boxes in Fig. 8) both have broadly chondritic compositions over nearly 200 Ma of formation. This consistent chondritic signature is also characteristic of the best constrained Hf isotope data in other Eoarchean terranes.

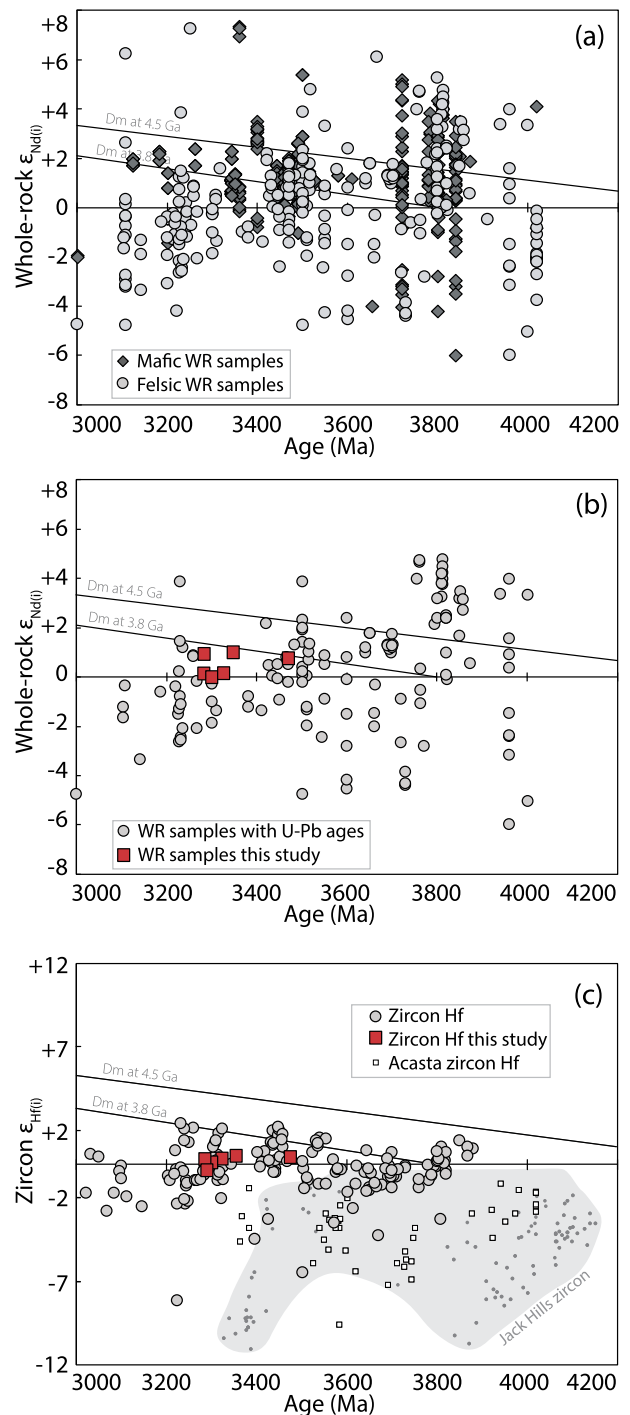


Fig. 8. Global compilation of initial Hf and Nd isotope compositions of crustal rocks, between 4.2 and 3.0 Ga. A) initial bulk rock Nd isotope values, B) initial bulk rock Nd isotope values for samples with corresponding zircon U-Pb ages, and C) initial Hf isotope values determined from zircon. Red boxes on plots (B) and (C) show the compositions of rocks of this study. Data sources for these plots are given in supplementary file 8. Included in this compilation are rocks from the Pilbara and Kaapvaal cratons, the Acasta Gneiss Complex, the Saglek Block of NE Canada, the Isua gneisses of SW Greenland, Nuvvuagittuq, and Minnesota River Valley gneisses (references given in the Supplementary file 8). Note that the Hf and Nd panels are drawn at the same scale (i.e. $\epsilon_{\text{Hf}} \sim 1.5 \epsilon_{\text{Nd}}$).

Given the potential for open system Sm-Nd behavior, we suggest the Hf isotope record provided by zircon components of ancient magmatic rocks provides the most unambiguous record of early silicate evolution of the Earth.

Notwithstanding this, the Nd isotope record can, in some circumstances, provide essential and unambiguous information on crust-mantle evolution, if an appropriate analytical approach is taken. Our data from the east Pilbara demonstrate that—for these samples—the Sm-Nd system has been closed and accurately records the broadly chondritic initial Nd isotope compositions of these rocks. This is in accord with Hf isotope data and supports a CHUR-like source reservoir. For samples that have been subjected to higher metamorphic grades, however, there is potential for Sm-Nd open system behavior through breakdown or recrystallization of less robust REE-rich phases (Hammerli et al., 2019; Fisher et al., 2020). In these cases—and especially where there is greater variation in Nd isotopes than Hf—it is essential to examine Sm-Nd isotope behavior on the mineral scale.

CRediT authorship contribution statement

R. Salerno: Conceptualization, Data curation, Formal analysis, Investigation, Resources, Validation, Visualization, Writing – original draft. **J. Vervoort:** Conceptualization, Funding acquisition, Methodology, Project administration, Resources, Supervision, Validation, Writing – original draft, Writing – review & editing. **C. Fisher:** Conceptualization, Methodology, Supervision, Validation, Writing – review & editing. **A. Kemp:** Conceptualization, Investigation, Resources, Writing – review & editing. **N. Roberts:** Resources, Writing – review & editing.

Declaration of competing interest

The authors declare that they have no known competing financial interests or personal relationships that could have appeared to influence the work reported in this paper.

Acknowledgements

We would like to acknowledge Charles Knaack and Chao Zhang at WSU for laboratory and technical support. We thank Basil Tikoff for helpful discussions and field logistic support. We would also like to thank the Brooks family of Marble Bar for their endless assistance during our Pilbara field seasons. JV would like to thank the H.R. Whiteley Center for providing a creative workspace. This project was supported with funding from the NSF grant EAR-2020831 to JV.

Appendix A. Supplementary material

Supplementary material related to this article can be found online at <https://doi.org/10.1016/j.epsl.2021.117139>.

References

- Amelin, Y., 2009. Sm-Nd and U-Pb systematics of single titanite grains. *Chem. Geol.* 261, 53–61. <https://doi.org/10.1016/j.chemgeo.2009.01.014>.
- Armstrong, R., 1981. Radiogenic isotopes: the case for crustal recycling on a near-steady-state no-continental-growth Earth. *Philos. Trans. R. Soc. Lond.* 301, 443–472.
- Arndt, N., Bruzack, G., Reischmann, T., 2001. The oldest continental and oceanic plateaus: geochemistry of basalts and komatiites of the Pilbara Craton, Australia. *Spec. Pap., Geol. Soc. Am.* 352, 359–387. <https://doi.org/10.1130/0-8137-2352-3.359>.
- Barker, F., 1979. Trondhjemite: definition, environment, and hypotheses of origin. In: Barker, F. (Ed.), *Trondhjemites, Dacites, and Related Rocks*. Elsevier, Amsterdam, pp. 1–12.
- Bauer, A.M., Fisher, C.M., Vervoort, J.D., Bowring, S.A., 2017. Coupled zircon Lu–Hf and U–Pb isotopic analyses of the oldest terrestrial crust, the >4.03 Ga Acasta Gneiss Complex. *Earth Planet. Sci. Lett.* 458, 37–48. <https://doi.org/10.1016/j.epsl.2016.10.036>.
- Bennett, V.C., Nutman, A.P., McCulloch, M.T., 1993. Nd isotopic evidence for transient, highly depleted mantle reservoirs in the early history of the Earth. *Earth Planet. Sci. Lett.* 119, 299–317. [https://doi.org/10.1016/0012-821X\(93\)90140-5](https://doi.org/10.1016/0012-821X(93)90140-5).
- Bennett, V.C., Brandon, A.D., Nutman, A.P., 2007. Coupled ^{142}Nd – ^{143}Nd isotopic evidence for hadean mantle dynamics. *Science* 318, 1907–1910. <https://doi.org/10.1126/science.1145928>.
- Bickle, M.J., Bettenay, L.F., Chapman, H.J., Groves, D.I., McNaughton, N.J., Campbell, I.H., de Laeter, J.R., 1993. Origin of the 3500–3300 Ma calc-alkaline rocks in the Pilbara Archaean: isotopic and geochemical constraints from the Shaw Batholith. *Precambrian Res.* 60, 117–149. [https://doi.org/10.1016/0301-9268\(93\)90047-6](https://doi.org/10.1016/0301-9268(93)90047-6).
- Bouvier, A., Vervoort, J.D., Patchett, P.J., 2008. The Lu–Hf and Sm–Nd isotopic composition of CHUR: constraints from unequilibrated chondrites and implications for the bulk composition of terrestrial planets. *Earth Planet. Sci. Lett.* 273, 48–57. <https://doi.org/10.1016/j.epsl.2008.06.010>.
- Bowring, S.A., Housh, T., 1995. The Earth's early evolution. *Science* 269, 1535–1540. <https://doi.org/10.1126/science.7667634>.
- Caro, G., Bourdon, B., Wood, B.J., Corgne, A., 2005. Trace-element fractionation in Hadean mantle generated by melt segregation from a magma ocean. *Nature* 436, 246–249. <https://doi.org/10.1038/nature03827>.
- DePaolo, D.J., 1981. Neodymium isotopes in the Colorado Front Range and crust-mantle evolution in the Proterozoic. *Nature* 291, 193–196. <https://doi.org/10.1038/291193a0>.
- de Witt, M., Roering, C., Hart, R.J., Armstrong, R., de Ronde, C., Green, R., Tredoux, M., Peberdy, E., Hart, R.A., 1992. Formation of the Archean continent. *Nature* 357, 553–562.
- Fisher, C.M., Vervoort, J.D., Hanchar, J.M., 2014. Guidelines for reporting zircon Hf isotopic data by LA-MC-ICPMS and potential pitfalls in the interpretation of these data. *Chem. Geol.* 363, 125–133. <https://doi.org/10.1016/j.chemgeo.2013.10.019>.
- Fisher, C.M., Vervoort, J.D., 2018. Using the magmatic record to constrain the growth of continental crust – the Eoarchean zircon Hf record of Greenland. *Earth Planet. Sci. Lett.* 488, 79–91. <https://doi.org/10.1016/j.epsl.2018.01.031>.
- Fisher, C.M., Bauer, A.M., Vervoort, J.D., 2020. Disturbances in the Sm–Nd isotope system of the Acasta Gneiss Complex—implications for the Nd isotope record of the early Earth. *Earth Planet. Sci. Lett.* 530, 115900. <https://doi.org/10.1016/j.epsl.2019.115900>.
- Gardiner, N.J., Hickman, A.H., Kirkland, C.L., Lu, Y., Johnson, T., Zhao, J.X., 2017. Processes of crust formation in the early Earth imaged through Hf isotopes from the East Pilbara Terrane. *Precambrian Res.* 297, 56–76. <https://doi.org/10.1016/j.precamres.2017.05.004>.
- Gaschnig, R., Vervoort, J., Lewis, R., Tikoff, B., 2011. Isotopic evolution of the Idaho Batholith and Challis Intrusive Province, Northern US Cordillera. *J. Petrol.* 52, 2397–2429. <https://doi.org/10.1093/ptrology/egr050>.
- Goudie, D., Fisher, C., Hanchar, J., Crowley, J., Ayers, J., 2014. Simultaneous in situ determination of U–Pb and Sm–Nd isotopes in monazite by laser ablation ICP-MS. *Geochim. Geophys. Geosyst.* 15, 2575–2600. <https://doi.org/10.1002/2014GC005431>.
- Gruau, G., Jahn, B.M., Glikson, A.Y., Davy, R., Hickman, A.H., Chauvel, C., 1987. Age of the Archean Talga-Talga Subgroup, Pilbara Block, Western Australia, and early evolution of the mantle: new SmNd isotopic evidence. *Earth Planet. Sci. Lett.* 85, 105–116. [https://doi.org/10.1016/0012-821X\(87\)90025-2](https://doi.org/10.1016/0012-821X(87)90025-2).
- Hammerli, J., Kemp, A.I.S., Spandler, C., 2014. Neodymium isotope equilibration during crustal metamorphism revealed by in situ microanalysis of REE-rich accessory minerals. *Earth Planet. Sci. Lett.* 392, 133–142. <https://doi.org/10.1016/j.epsl.2014.02.018>.
- Hammerli, J., Kemp, A.I.S., Whitehouse, M.J., 2019. In situ trace element and Sm–Nd isotope analysis of accessory minerals in an Eoarchean tonalitic gneiss from Greenland: Implications for Hf and Nd isotope decoupling in Earth's ancient rocks. *Chem. Geol.* 524, 394–405. <https://doi.org/10.1016/j.chemgeo.2019.06.025>.
- Hasenstab, E., Tusch, J., Schnabel, C., Marien, C.S., Van Kranendonk, M.J., Smithies, H., Howard, H., Maier, W.D., Münker, C., 2021. Evolution of the early to late Archean mantle from Hf–Nd–Ce isotope systematics in basalts and komatiites from the Pilbara Craton. *Earth Planet. Sci. Lett.* 553, 116627. <https://doi.org/10.1016/j.epsl.2020.116627>.
- Hickman, A.H., 2012. Review of the Pilbara Craton and Fortescue Basin, Western Australia: crustal evolution providing environments for early life. *Isl. Arc* 21, 1–31. <https://doi.org/10.1111/j.1440-1738.2011.00783.x>.
- Hickman, A.H., Van Kranendonk, M., 2012. Early Earth evolution: evidence from the 3.5–1.8 Ga Geological history of the Pilbara region of Western Australia. *Episodes* 35, 283–297.
- Hoffmann, J.E., Münker, C., Polat, A., König, S., Mezger, K., Rosing, M.T., 2010. Highly depleted Hadean mantle reservoirs in the sources of early Archean arc-like rocks, Isua supracrustal belt, southern West Greenland. *Geochim. Cosmochim. Acta* 74, 7236–7260. <https://doi.org/10.1016/j.gca.2010.09.027>.
- Hoffmann, J.E., Münker, C., Polat, A., Rosing, M.T., Schulz, T., 2011. The origin of decoupled Hf–Nd isotope compositions in Eoarchean rocks from southern West Greenland. *Geochim. Cosmochim. Acta* 75, 6610–6628. <https://doi.org/10.1016/j.gca.2011.08.018>.
- Hoffmann, J.E., Wilson, A., 2017. The origin of highly radiogenic Hf isotope compositions in 3.33 Ga Comondale komatiite lavas (South Africa). *Chem. Geol.* 455, 6–21. <https://doi.org/10.1016/j.chemgeo.2016.10.010>.
- Jacobsen, S., Wasserburg, G., 1979. The mean age of crustal reservoirs. *J. Geophys. Res.* 84, 7411–7427.

- Jahn, B.M., Glikson, A.Y., Peucat, J.J., Hickman, A.H., 1981. REE geochemistry and isotopic data of Archean silicic volcanics and granitoids from the Pilbara Block, Western Australia: implications for the early crustal evolution. *Geochim. Cosmochim. Acta* 45, 1633–1652. [https://doi.org/10.1016/S0016-7037\(81\)80002-6](https://doi.org/10.1016/S0016-7037(81)80002-6).
- Johnson, T.A., Vervoort, J.D., Ramsey, M.J., Aleinikoff, J.N., Southworth, S., 2018. Constraints on the timing and duration of orogenic events by combined Lu-Hf and Sm-Nd geochronology: an example from the Grenville orogeny. *Earth Planet. Sci. Lett.* 501, 152–164.
- Kemp, A.I.S., Foster, G.L., Scherstén, A., Whitehouse, M.J., Darling, J., Storey, C., 2009. Concurrent Pb-Hf isotope analysis of zircon by laser ablation multi-collector ICP-MS, with implications for the crustal evolution of Greenland and the Himalayas. *Chem. Geol.* 261, 244–260. <https://doi.org/10.1016/j.chemgeo.2008.06.019>.
- Kemp, A.I.S., Wilde, S.A., Hawkesworth, C.J., Coath, C.D., Nemchin, A., Pidgeon, R.T., Vervoort, J.D., DuFrane, S.A., 2010. Hadean crustal evolution revisited: new constraints from Pb-Hf isotope systematics of the Jack Hills zircons. *Earth Planet. Sci. Lett.* 296, 45–56. <https://doi.org/10.1016/j.epsl.2010.04.043>.
- Kemp, A.I.S., Hickman, A.H., Kirkland, C.L., Vervoort, J.D., 2015. Hf isotopes in detrital and inherited zircons of the Pilbara Craton provide no evidence for Hadean continents. *Precambrian Res.* 261, 112–126. <https://doi.org/10.1016/j.precamres.2015.02.011>.
- Kemp, A., Vervoort, J., Bjorkman, K., Iaccheri, L., 2017. Hafnium Isotope characteristics of Palaeoarchean Zircon OG1/OGC from the Owens Gully Diorite, Pilbara Craton, Western Australia. *Geostand. Geoanal. Res.* 41, 659–673. <https://doi.org/10.1111/ggr.12182>.
- Kemp, A.I.S., Whitehouse, M.J., Vervoort, J.D., 2019. Deciphering the zircon Hf isotope systematics of Eoarchean gneisses from Greenland: implications for ancient crust-mantle differentiation and Pb isotope controversies. *Geochim. Cosmochim. Acta* 250, 76–97. <https://doi.org/10.1016/j.gca.2019.01.041>.
- Lugmair, G., Marti, K., 1978. Lunar initial $^{143}\text{Nd}/^{144}\text{Nd}$: differential evolution of the lunar crust and mantle. *Earth Planet. Sci. Lett.* 39, 349–357. [https://doi.org/10.1026/002-821X\(78\)90021-3](https://doi.org/10.1026/002-821X(78)90021-3).
- McCulloch, M.T., 1987. Sm-Nd isotopic constraints on the evolution of Precambrian crust in the Australian continent. In: Kroner, A. (Ed.), *Proterozoic Lithospheric Evolution*, Vol. 17. American Geophysical Union, Washington DC, pp. 115–130.
- McCulloch, M.T., Bennett, V.C., 1994. Progressive growth of the Earth's continental crust and depleted mantle: geochemical constraints. *Geochim. Cosmochim. Acta* 58, 4717–4738. [https://doi.org/10.1016/0016-7037\(94\)90203-8](https://doi.org/10.1016/0016-7037(94)90203-8).
- Moorbath, S., Whitehouse, M., Kamber, B., 1997. Extreme Nd-isotope heterogeneity in the early Archaean—fact or fiction? Case histories from northern Canada and West Greenland. *Chem. Geol.* 135, 213–231. [https://doi.org/10.1016/S0009-2541\(96\)00117-9](https://doi.org/10.1016/S0009-2541(96)00117-9).
- Murphy, D., Rizo, H., O'Neil, J., Hepple, R., Weimer, D., Kemp, A., Vervoort, J., 2021. Combined Sm-Nd, Lu-Hf, and ^{142}Nd study of Paleoproterozoic basalts from the East Pilbara Terrane, Western Australia. *Chem. Geol.* 578. <https://doi.org/10.1016/j.chemgeo.2021.120301>.
- Nebel, O., Campbell, I., Sossi, P., Van Kranendonk, M., 2014. Hafnium and iron isotopes in early Archaean komatiites record a plume-driven convection cycle in the Hadean Earth. *Earth Planet. Sci. Lett.* 397, 111–120. <https://doi.org/10.1016/j.epsl.2014.04.028>.
- Nelson, D.R., 1999. *Compilation of geochronology data*. Rep., Geol. Surv. West. Aust.
- O'Neil, J., Boyet, M., Carlson, R.W., Paquette, J.L., 2013. Half a billion years of reworking of Hadean mafic crust to produce the Nuvvuagittuq Eoarchean felsic crust. *Earth Planet. Sci. Lett.* 379, 13–25. <https://doi.org/10.1016/j.epsl.2013.07.030>.
- Petersson, A., Kemp, A.I.S., Hickman, A.H., Whitehouse, M.J., Martin, L., Gray, C.M., 2019. A new 3.59 Ga magmatic suite and a chondritic source to the east Pilbara Craton. *Chem. Geol.* 511, 51–70. <https://doi.org/10.1016/j.chemgeo.2019.01.021>.
- Petersson, A., Kemp, A.I.S., Gray, C.M., Whitehouse, M.J., 2020. Formation of early Archaean Granite-Greenstone Terranes from a globally chondritic mantle: insights from igneous rocks of the Pilbara Craton, Western Australia. *Chem. Geol.* 551, 119757. <https://doi.org/10.1016/j.chemgeo.2020.119757>.
- Rizo, H., Boyet, M., Blichert-Toft, J., Rosing, M., 2011. Combined Nd and Hf isotope evidence for deep-seated source of Isua lavas. *Earth Planet. Sci. Lett.* 312, 267–279. <https://doi.org/10.1016/j.epsl.2011.10.014>.
- Rizo, H., Boyet, M., Blichert-Toft, J., O'Neil, J., Rosing, M.T., Paquette, J.L., 2012. The elusive Hadean enriched reservoir revealed by ^{142}Nd deficits in Isua Archaean rocks. *Nature* 491, 96–100. <https://doi.org/10.1038/nature11565>.
- Smithies, R.H., ÿon, D.C., Van Kranendonk, M.J., Hickman, A.H., 2007. *Geochemistry of volcanic units of the northern Pilbara Craton, Western Australia*. Rep., Geol. Surv. West. Aust.
- Smithies, R.H., Champion, D.C., Van Kranendonk, M.J., 2009. Formation of Paleoproterozoic continental crust through infracrustal melting of enriched basalt. *Earth Planet. Sci. Lett.* 281, 298–306. <https://doi.org/10.1016/j.epsl.2009.03.003>.
- Söderlund, U., Patchett, P.J., Vervoort, J.D., Isachsen, C.E., 2004. The ^{176}Lu decay constant determined by Lu-Hf and U-Pb isotope systematics of Precambrian mafic intrusions. *Earth Planet. Sci. Lett.* 219, 311–324. [https://doi.org/10.1016/S0012-821X\(04\)00012-3](https://doi.org/10.1016/S0012-821X(04)00012-3).
- Tessalina, S., Bourdon, B., Van Kranendonk, M., Birck, J., Philippot, P., 2010. Influence of Hadean crust evidence in basalts and cherts from the Pilbara Craton. *Nat. Geosci.* 3, 214–217. <https://doi.org/10.1038/ngeo772>.
- Tympel, J., Hergt, J., Maas, R., Woodhead, J., Greig, A., Bolhar, R., Powell, R., 2021. Mantle like Hf-Nd isotope signatures in 3.5 Ga greenstones: no evidence for Hadean crust beneath the East Pilbara Craton. *Chem. Geol.* 576. <https://doi.org/10.1016/j.chemgeo.2021.120273>.
- Van Kranendonk, M., Hickman, A., Smithies, H., Nelson, D., 2002. *Geology and Tectonic Evolution of the Archean North Pilbara Terrain, Pilbara Craton, Western Australia*. Econ. Geol. 97, 695–732. <https://doi.org/10.2113/gsecongeo.97.4.695>.
- Vervoort, J.D., Patchett, P.J., Gehrels, G.E., Nutman, A.P., 1996. Constraints on early Earth differentiation from hafnium and neodymium isotopes. *Nature*. <https://doi.org/10.1038/379624a0>.
- Vervoort, J.D., Blichert-Toft, J., 1999. Evolution of the depleted mantle: Hf isotope evidence from juvenile rocks through time. *Geochim. Cosmochim. Acta* 63, 533–556. [https://doi.org/10.1016/S0016-7037\(98\)00274-9](https://doi.org/10.1016/S0016-7037(98)00274-9).
- Vervoort, J.D., Patchett, P.J., Blichert-Toft, J., Albarède, F., 1999. Relationships between Lu-Hf and Sm-Nd isotopic systems in the global sedimentary system. *Earth Planet. Sci. Lett.* 168, 79–99. [https://doi.org/10.1016/S0012-821X\(99\)00047-3](https://doi.org/10.1016/S0012-821X(99)00047-3).
- Vervoort, J.D., Plank, T., Prytulak, J., 2011. The Hf-Nd isotopic composition of marine sediments. *Geochim. Cosmochim. Acta* 75, 5903–5926. <https://doi.org/10.1016/j.gca.2011.07.046>.
- Vervoort, J.D., 2014. *Evolution of the depleted mantle and growth of the continental crust: an early beginning or a slow start?* In: *European Geophysical Union Abstracts*. 14683.
- Vervoort, J.D., Kemp, A.I.S., 2016. Clarifying the zircon Hf isotope record of crust-mantle evolution. *Chem. Geol.* 425, 65–75. <https://doi.org/10.1016/j.chemgeo.2016.01.023>.
- Whitehouse, M., Kamber, B., Moorbath, S., 1999. Age significance of U-Th-Pb data from early Archaean rocks of Greenland – a reassessment based on combined ion-microprobe and imaging studies. *Chem. Geol.* 160, 201–224. [https://doi.org/10.1016/S0009-2541\(99\)00066-2](https://doi.org/10.1016/S0009-2541(99)00066-2).
- Williams, I.R., Bagas, L., 2007. *Geology of the Mount Edgar 1:100,000 Sheet*. Geological Survey of Western Australia Explanatory Notes.
- Williams, I.S., Collins, W.J., 1990. Granite-greenstone terranes in the Pilbara Block, Australia, as coeval volcano-plutonic complexes; evidence from U-Pb zircon dating of the Mount Edgar Batholith. *Earth Planet. Sci. Lett.* 97, 41–53. [https://doi.org/10.1016/0012-821X\(90\)90097-H](https://doi.org/10.1016/0012-821X(90)90097-H).
- Zeh, A., Gerdes, A., Klemd, R., Barton, J.M., 2007. Archaean to proterozoic crustal evolution in the central zone of the Limpopo Belt (South Africa-Botswana): constraints from combined U-Pb and Lu-Hf isotope analyses of zircon. *J. Petrol.* 48 (8), 1605–1639. <https://doi.org/10.1093/ptrology/egm032>.